Amplitude scaling of a static wrinkle at an oil-air interface created by dielectrophoresis forces

C. V. Brown,[a] W. Al-Shabib, G. G. Wells, G. McHale, and M. I. Newton
School of Science and Technology, Nottingham Trent University, Erasmus Darwin Building, Clifton Lane, Clifton, Nottingham NG11 8NS, United Kingdom

(Received 3 September 2010; accepted 18 November 2010; published online 13 December 2010)

Dielectrophoresis forces have been used to create a static periodic wrinkle with a sinusoidal morphology on the surface of a thin layer of 1-decanol oil. The surface deformation occurs when a voltage V is applied between adjacent coplanar strip electrodes in an interdigitated array onto which the oil film is coated. It has been shown experimentally that the peak-to-peak amplitude A of the wrinkle scales according to the functional form $A \propto V^2 \exp(-\alpha \bar{h}/p)$ for a range of oil film thicknesses $\bar{h}$ (between 15 and 50 μm) and wrinkle pitches p (160, 240, and 320 μm). © *2010 American Institute of Physics*. [doi:10.1063/1.3525708]

Dielectrophoresis forces act on any polarizable dielectric material that is in a region containing nonuniform electric fields. The magnitude of the force is related to the gradient of the electric field and it acts in the direction of the increase in magnitude of the electric field.[1–3] Particle dielectrophoresis is used in the analysis and separation of biological particles such as cells.[2,4] In liquid dielectrophoresis, the tendency of a dielectric liquid to collect in regions of highest nonuniform electric field intensity has been exploited in microscale fluid actuation for lab-on-a-chip applications.[5,6] We have recently reported how the concept of liquid dielectrophoresis can be used to create a static periodic "wrinkle" deformation at the free surface of a thin film of oil in air[7] to create a voltage programmable optical effect. The current investigation focuses on establishing the underlying physics of how the peak-to-peak amplitude A of the wrinkle scales with the average thickness $\bar{h}$ of the oil film and the pitch p of the wrinkle.

A cross section through the device geometry is shown in Fig. 1(a). A two-dimensional array of coplanar strip electrodes is patterned on top of a glass substrate. The electrode architecture was fabricated using standard photolithography and etching techniques from a continuous layer of indium tin oxide of thickness 25 nm and resistivity 100 Ω/sq (Praezisions Glas and Optik GmbH, Iserlohn, Germany). The electrodes were configured in an interdigitated geometry in which alternate electrodes in the array were electrically connected so that neighboring electrodes could be separately biased, as shown in Fig. 1(a). The electrode widths w were equal to the spacing between the electrodes. The electrodes were coated with a 0.5 μm thick dielectric layer of SU8 photoresist (MicroChem Corp., MA, USA), which provided planarization and ensured electrical isolation between neighboring electrodes.

1-decanol was applied to the device using a Gilsen 0.1–2 μl dispensing pipette. When a potential difference greater than 30 V (10 kHz squarewave) was applied between the interdigitated electrodes, the oil spreads into a thin film in the x-y plane with uniform thickness covering the 5 mm $\times$5 mm square area immediately above the electrodes. Increasing the voltage further resulted in the appearance of a sinusoidal periodic wrinkle at the oil-air interface. The pitch p of the wrinkle was equal to twice the electrode width, $p=2w$, and this was determined by the fabricated electrode dimensions which, in this study, were 160, 240, or 320 μm. The spreading of the oil into a uniform film and the creation of the surface wrinkle at the oil-air interface can both be understood as a consequence of the dielectrophoresis forces. The interdigitated electrode geometry generates highly nonuniform "fringing" electric fields in the region immediately above the electrode array and the fluid flows and spreads to occupy this region. The highest nonuniform electric field intensities are found between the electrodes and the oil collects preferentially in these regions immediately above the electrode gaps, which creates the surface wrinkle morphology.

The wrinkle amplitude $A(V)$ and average oil film thickness $\bar{h}$ were both measured from the displacement of tilt interference fringes when the sample was placed in one arm

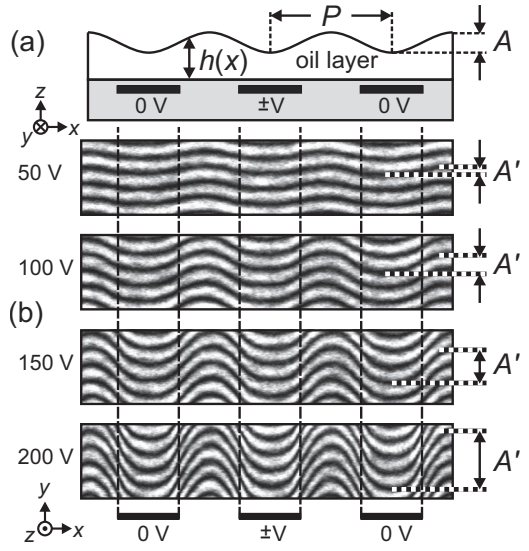

FIG. 1. (a) Schematic depiction of the device geometry showing a cross section through a thin film of oil that lies in the x-y plane. Dielectrophoresis forces produce a sinusoidal wrinkle at the air-oil interface. (b) When the device is placed in a Mach–Zehnder interferometer, the wrinkle produces a displacement of tilt interference fringes at horizontal position x that is directly proportional to the thickness of the oil film $h(x)$.

[a]Tel.: 44(0)115-8483184. Electronic mail: carl.brown@ntu.ac.uk.

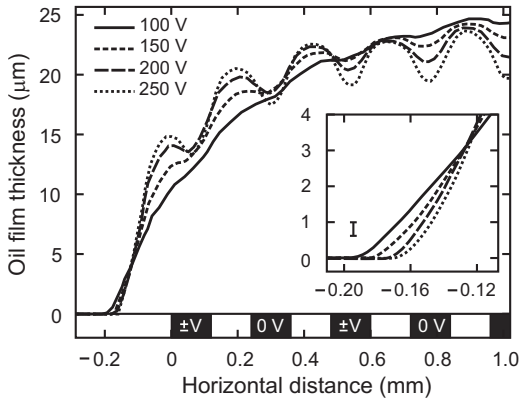

FIG. 2. The oil film thickness profile at the edge of a spread oil film for applied voltages of 100 V (solid line), 150 V (medium dashed line), 200 V (long dashed line), and 250 V (dotted line). The solid rectangles at the lower edge of the figure show the positions of the electrodes of width 120 μm that are buried beneath a 0.5 μm thick layer of dielectric (SU8 photoresist). An expanded graph in the region at the three phase contact line is shown inset. The estimated experimental accuracy is shown by the vertical line in the inset figure.

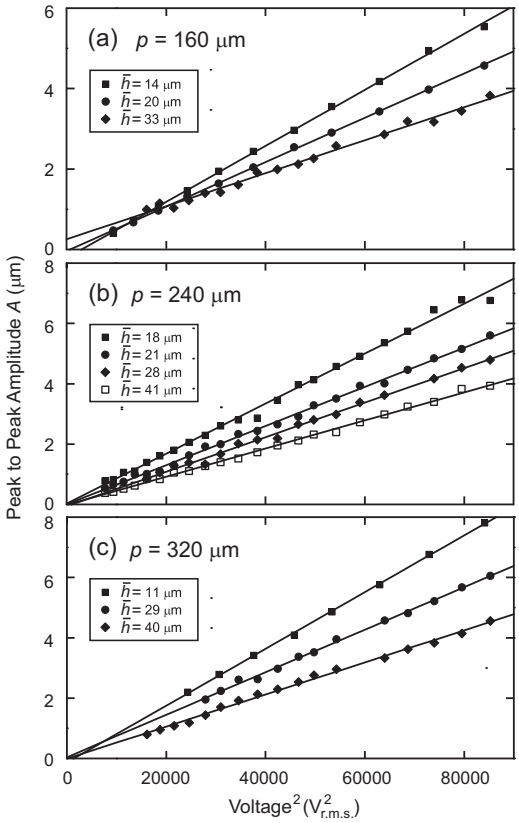

FIG. 3. The peak-to-peak amplitude A of the wrinkle produced by dielectrophoresis forces at the surface of the oil film is plotted as a function of the square of the rms value of the ac voltage. Measurements were performed on devices with three different wrinkle pitches: (a) $p=160$ μm, (b) $p=240$ μm, and (c) $p=320$ μm. At each pitch value, data are shown for a number of different average oil film thicknesses $\bar{h}$. The solid lines show linear regression fits to the data for each different set of p and $\bar{h}$ values.

of a Mach–Zehnder interferometer. Figure 1(b) shows the appearance of the interference fringes for a device with electrodes of width $w=120$ μm ($p=240$ μm) and average film thickness $\bar{h}=18.2$ μm when the voltage between adjacent electrodes was set at 50, 100, 150, and 200 V (10 kHz squarewave). The vertical displacement $y(x)$ of the fringes at a given position x along the oil layer is determined by the optical path length of transmitted light at that position, which depends on the thickness of the oil layer $h(x)$ at that position, the wavelength of light λ (633 nm), and the difference between the refractive index of 1-decanol oil n_{oil} (1.438) and the refractive index of air n_{air}. The fringe displacement $y(x)$ expressed as a fraction of the (constant) distance Δy between two adjacent fringes is given by $y(x)/\Delta y=[h(x)/\lambda]\cdot(n_{oil}-n_{air})$. The peak-to-peak amplitude of the surface wrinkle $A=h_{peak}-h_{trough}$ can be found directly from the difference in the displacements of the fringes at a peak and at a trough, respectively, indicated by the distance A' in Fig. 1(b).

Figure 2 shows the oil film thickness profiles $h(x)$ at the edge of an oil film that coats electrodes of width $w=120$ μm. The horizontal x coordinate is measured from the edge of the electrodes, where the positions of the electrodes are shown by the solid rectangles at the lower edge of the graph. The thickness profiles are shown when the 10 kHz squarewave voltage between adjacent electrodes was set at 100, 150, 200, and 250 V. As the voltage increases, the gradient of the oil film thickness profile becomes steeper in the region at the edge of the electrodes. An expanded view of profile in the region of the oil-air-photoresist contact line, or triple line, is shown in the inset of Fig. 2. The limit of experimental accuracy, shown by the cross in the inset figure, was estimated to be ± 0.2 μm in the determination of the height profile $h(x)$ due to the finite width of the interference fringes. The oil film thickness is shown as 0 in the region where $x \ll 0$ in Fig. 2. This is not necessarily the case but any uniform oil layer cannot be detected since the measurement involves the relative shift of interference fringes. For all voltage values, the oil film thickness profiles show a point of inflexion near the edge of the spread films.[8,9] As the voltage is increased, the triple line recedes slightly toward the region covered by the electrodes. This is accompanied by an increase in the contact angle (defined by extrapolation from the point of inflexion) from 3.1° at 100 V to 6.1° at 250 V.

The average oil film thickness $\bar{h}$ is found from the midpoints between the peaks and troughs of the surface wrinkle at least 1 mm from the electrode edge. The values of $\bar{h}$ in Fig. 2 are 24.6 μm at 100 V, 23.9 μm at 150 V, 22.7 μm at 200 V, and 21.8 μm at 250 V. The thickness of the spread oil film was determined by the amount of oil dispensed onto the device and this was generally found to remain constant to within $\pm 6\%$ over the range of voltages used. Taking into account this variation and the variations in uniformity of the spread oil film found by measuring the oil film thickness at different edges gave an estimated random error of $\pm 8\%$ on the value of $\bar{h}$.

In Fig. 3 the peak-to-peak amplitude A of the wrinkle at the oil-air interface is plotted as a function of the square of the rms value of voltage (which equals the peak value for the 10 kHz squarewave voltage waveform used) for three different wrinkle pitches: (a) $p=160$ μm, (b) $p=240$ μm, and (c) $p=320$ μm. Data are shown for several different average oil film thicknesses $\bar{h}$ at each pitch value. A clear linear relationship between A and V^2 is exhibited for the range of thickness and pitch values, for which the ratio $\bar{h}/p$ varies in the range from $\bar{h}/p=0.035$ to 0.206. The data in Fig. 3 represent a sample from a total of 24 separate experiments across the

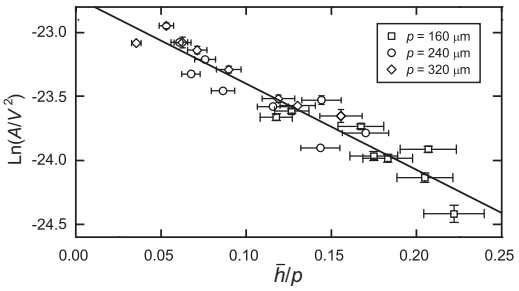

FIG. 4. The natural logarithm of the gradient of the linear regression fit to the wrinkle amplitude vs voltage squared relationships is plotted against the ratio $\bar{h}/p$ for static wrinkles at the oil-air interface with a pitch p on an oil film with average thickness $\bar{h}$.

range of values of $\bar{h}/p$. Linear regression fits to the A versus V^2 curves (shown by the solid lines in Fig. 3) yielded an average standard error of 2.6% on the gradients and the intercepts with the amplitude axis lay within ± 0.3 μm of the origin. In Fig. 4 the natural logarithms of the gradient values of the A versus V^2 curves are plotted against the corresponding values of the ratio $\bar{h}/p$. The linear regression fit to the experimental data (solid line) corresponds to the functional form $A=kV^2 \exp(-\alpha\bar{h}/p)$ where $\alpha=6.8\pm0.5$ and with the constant of proportionality $k=(1.4\pm0.1)\times10^{-10}$ m.

The corrugation of the oil-air interface can be intuitively understood by considering the increase in its area and in the associated surface free energy, $W_S=\gamma_{LV}\int[1+(\nabla y)^2]^{1/2}dS$, where γ_{LV} is the oil-air interfacial surface tension. For a sinusoidal surface deformation described by $h(x)=\bar{h}+\frac{1}{2}A\cos(2\pi x/p)$, the excess surface free energy due to the wrinkle is given by $W_S \propto \gamma_{LV}A^2/p$ (per unit length in the y direction) in the limit $A \ll p$. This increased interfacial energy is balanced by the decrease in the electrostatic energy $W_E=\frac{1}{2}\Delta C\cdot V^2$, where ΔC is the change in capacitance produced by some of the oil redistributing and collecting in the regions between the electrodes. Since the 1-decanol oil has a dielectric constant of 8.1 and air has a much lower dielectric constant of 1, the appearance of a nonuniform layer of oil can balance the change in surface free energy caused by the wrinkle. The potential due to an interdigitated electrode array decays exponentially with distance z from the electrodes with the relationship $V(z)\sim V_O \exp(-\pi z/p)$ (Refs. 10–14) to first order giving $V^2(\bar{h})\sim V_O^2 \exp(-2\pi\bar{h}/p)$ at the oil-air interface z-position of the wrinkle, $z=\bar{h}$. The change in the capacitance due to the appearance of wrinkle is given by $\Delta C \propto \varepsilon_O\varepsilon_{oil}\delta[h(x)/p]\sim\varepsilon_O\varepsilon_{oil}(A/p)$ to first order and so the change in electrostatic energy is given by $W_E \sim \frac{1}{2}\varepsilon_O\varepsilon_{oil}(A/p)V_O^2 \exp(-2\pi\bar{h}/p)$ (per unit length in the y direction). Minimizing the total energy $W=W_S-W_E$ with respect to the peak-to-peak amplitude A of the wrinkle yields the expression $A\propto(\varepsilon_O\varepsilon_{oil}/4\gamma_{LV})V_O^2 \exp(-2\pi\bar{h}/p)$.

The above consideration of the balance between the surface tension and the electrostatic energies reproduces the experimentally observed scaling relationship. Moreover, it predicts a coefficient in the argument of the exponential of $2\pi=6.28$, which agrees with the experimentally observed value of $\alpha=6.8\pm0.5$ to within one standard error. This approach also identifies the dependences on the key material parameters of the oil, γ_{LV} and ε_{oil}. The form used for the electrostatic energy above can be justified analytically by performing the integration $W_E=\frac{1}{2}\varepsilon_O\varepsilon_{oil}\int\int\nabla^2V(x,z)dzdx$ between the limits $z=0$ to $z=h(x)$ and $x=-p$ to $x=p$ and using a suitable Fourier series approximation for the potential profile $V(x,z)$.[12–14] The full quantitative analysis requires a knowledge of the nonuniform electrical potential profile produced by the electrode geometry taking into account the complexities introduced by the distortion of the electric field at the oil-air boundary; neglecting this boundary results in an overestimation in the argument of the exponential of a factor of 2.[7]

At lower pitch values, the device has potential application for use as an electro-optical modulator through operation as a voltage programmable phase grating in which the refractive index mismatch between the periodically deformed oil surface and the surrounding air produces tunable diffraction of transmitted light.[7] Tunable phase grating devices have previously been produced based on a solid elastomeric layer coated with a deformable mirror,[15] birefringent nematic liquid crystal layers,[16,17] and using mechanical actuation to create buckling instabilities on a stretched thin polymer film.[18–20] The tunability of the wrinkle amplitude on the liquid surface has potential applications in controlling thermal cooling, since a wrinkled surface is a more efficient thermal radiator, and for low-cost sensing devices with optical read-out, since the amplitude of the wrinkle depends on the physical properties (surface tension and dielectric constant) of the liquid. The ability to electrically actuate the spreading of a liquid into a thin film has potential applications for voltage controlled coating and lubrication.

The authors gratefully acknowledge Dr. J. Fyson at Kodak European Research and Dr. C. L. Trabi at Nottingham Trent University for stimulating discussions. G.G.W. gratefully acknowledges Kodak European Research, Ltd. and the EPSRC/DTI COMIT Faraday Partnership for funding.

[1] H. Pellat, Acad. Sci., Paris, C. R. **119**, 691 (1895).
[2] H. A. Pohl, *Dielectrophoresis: The Behaviour of Neutral Matter in Non-Uniform Electric Fields*, Cambridge Monographs on Physics (Cambridge University Press, Cambridge, 1978).
[3] P. Lorrain and D. R. Corson, *Electromagnetic Fields and Waves*, 2nd ed. (Freeman, San Francisco, 1970).
[4] R. Pethig, Crit. Rev. Biotechnol. **16**, 331 (1996).
[5] T. B. Jones, J. Electrost. **51–52**, 290 (2001).
[6] T. B. Jones, M. Gunji, M. Washizu, and M. J. Feldman, J. Appl. Phys. **89**, 1441 (2001).
[7] C. V. Brown, G. G. Wells, M. I. Newton, and G. McHale, Nat. Photonics **3**, 403 (2009).
[8] Y. Xu, N. Zhang, W.-J. Yang, and C. M. Vest, Exp. Fluids **2**, 142 (1984).
[9] K. H. Guo, T. Uemura, and W.-J. Yang, Appl. Opt. **24**, 2655 (1985).
[10] H. Engan, IEEE Trans. Electron Devices **16**, 1014 (1969).
[11] M. Feldmann, Ann. Telecommun. **28**, 352 (1973).
[12] H. Morgan, A. Izquierdo, D. Bakewell, N. G. Green, and A. Ramos, J. Phys. D **34**, 1553 (2001).
[13] M. W. den Otter, Sens. Actuators, A **96**, 140 (2002).
[14] D. E. Chang, S. Loire, and I. Mezić, J. Phys. D **36**, 3073 (2003).
[15] R. Gerhard-Multhaupt, Displays **12**, 115 (1991).
[16] B. Apter, U. Efron, and E. Bahat-Treidel, Appl. Opt. **43**, 11 (2004).
[17] J. N. Eakin, Y. Xie, R. A. Pelcovits, M. D. Radcliffe, and G. P. Crawford, Appl. Phys. Lett. **85**, 1671 (2004).
[18] N. Bowden, S. Brittain, A. G. Evans, J. W. Hutchinson, and G. M. Whitesides, Nature (London) **393**, 146 (1998).
[19] N. Bowden, W. T. S. Huck, K. E. Paul, and G. M. Whitesides, Appl. Phys. Lett. **75**, 2557 (1999).
[20] T. Ohzono, H. Monobe, R. Yamaguchi, Y. Shimizu, and H. Yokoyama, Appl. Phys. Lett. **95**, 014101 (2009).